Visualization of semileptonic form factors from lattice QCD

C. Bernard,[1] C. DeTar,[2] M. Di Pierro,[3] A. X. El-Khadra,[4] R. T. Evans,[4] E. D. Freeland,[5] E. Gamiz,[4] Steven Gottlieb,[6] U. M. Heller,[7] J. E. Hetrick,[8] A. S. Kronfeld,[9] J. Laiho,[1] L. Levkova,[2] P. B. Mackenzie,[9] M. Okamoto,[9] M. B. Oktay,[2] J. N. Simone,[9] R. Sugar,[10] D. Toussaint,[11] and R. S. Van de Water[12]

(Fermilab Lattice and MILC Collaborations)

[1]*Department of Physics, Washington University, St. Louis, Missouri, USA*
[2]*Physics Department, University of Utah, Salt Lake City, Utah, USA*
[3]*School of Computer Science, Telecommunications and Information Systems, DePaul University, Chicago, Illinois, USA*
[4]*Physics Department, University of Illinois, Urbana, Illinois, USA*
[5]*Liberal Arts Department, The School of the Art Institute of Chicago, Chicago, Illinois, USA*
[6]*Department of Physics, Indiana University, Bloomington, Indiana, USA*
[7]*American Physical Society, Ridge, New York, USA*
[8]*Physics Department, University of the Pacific, Stockton, California, USA*
[9]*Fermi National Accelerator Laboratory, Batavia, Illinois, USA*
[10]*Department of Physics, University of California, Santa Barbara, California, USA*
[11]*Department of Physics, University of Arizona, Tucson, Arizona, USA*
[12]*Physics Department, Brookhaven National Laboratory, Upton, New York, USA*
(Received 16 June 2009; published 21 August 2009)

Comparisons of lattice-QCD calculations of semileptonic form factors with experimental measurements often display two sets of points, one each for lattice QCD and experiment. Here we propose to display the output of a lattice-QCD analysis as a curve and error band. This is justified, because lattice-QCD results rely in part on fitting, both for the chiral extrapolation and to extend lattice-QCD data over the full physically allowed kinematic domain. To display an error band, correlations in the fit parameters must be taken into account. For the statistical error, the correlation comes from the fit. To illustrate how to address correlations in the systematic errors, we use the Bećirević-Kaidalov parametrization of the $D \to \pi l \nu$ and $D \to K l \nu$ form factors, and an analyticity-based fit for the $B \to \pi l \nu$ form factor f_+.

DOI: 10.1103/PhysRevD.80.034026 PACS numbers: 13.20.Fc, 12.38.Gc, 13.20.He

The past several years have witnessed considerable improvement in our understanding of semileptonic decays of D and B mesons. Measurements have advanced in accuracy from 6%–20% on the normalization [1–3] and ~10% on the shape [4] to ~1% on both [5]. Meanwhile, *ab initio* calculations in QCD with lattice gauge theory have become realistic [6–9], now incorporating the effects of sea quarks that were omitted in earlier work [10–14]. In this article, we discuss how to present both together, so that the agreement (or, in principle, lack thereof) is easy to assess.

We focus on reactions mediated by electroweak vector currents, leading to pseudoscalar mesons, π or K, in the final state. At the quark level, a heavy quark h decays into a daughter quark d (not necessarily the down quark), with a spectator antiquark $\bar{q}$. Writing the decay $H \to P l \nu$, the form factors are defined by

$$\langle P|V^\mu|H\rangle = f_+(q^2)(p_H + p_P - \Delta)^\mu + f_0(q^2)\Delta^\mu, \quad (1)$$

where $q = p_H - p_P$ is the 4-momentum of the lepton system, and $\Delta^\mu = (p_H + p_P)\cdot q q^\mu/q^2 = (m_H^2 - m_P^2)q^\mu/q^2$. Equation (1) is general, applying to $K \to \pi l \nu$ as well as to D and B decays. For lattice QCD, it is more convenient to express the transition matrix element as

$$\langle P|V^\mu|H\rangle = \sqrt{2m_H}[v^\mu f_\parallel(E) + p_\perp^\mu f_\perp(E)], \quad (2)$$

where $v = p_H/m_H$, and $p_\perp = p_P - Ev$ and $E = v \cdot p_P$ denote the 3-momentum and energy of the final-state meson in the rest frame of the initial state. The energy E is related to q^2 via

$$q^2 = m_H^2 + m_P^2 - 2m_H E. \quad (3)$$

Neglecting the lepton mass, $0 \le q^2 \le q^2_{\rm max} = (m_H - m_P)^2$ is kinematically allowed in the semileptonic decay.

The form factors $f_+(q^2)$ and $f_0(q^2)$ are related to $f_\parallel(E)$ and $f_\perp(E)$ by

$$f_+(q^2) = (2m_H)^{-1/2}[f_\parallel(E) + (m_H - E)f_\perp(E)], \quad (4)$$

$$f_0(q^2) = \frac{\sqrt{2m_H}}{m_H^2 - m_P^2}[(m_H - E)f_\parallel(E) - p_\perp^2 f_\perp(E)], \quad (5)$$

with Eq. (3) understood. Equations (4) and (5) imply $f_+(0) = f_0(0)$, as required in Eq. (1).

Two aspects of lattice-QCD calculations are important here. First (as in all lattice-QCD calculations), it is computationally demanding to have a spectator quark with mass as small as those of the up and down quarks;

for $P = \pi$ the same applies to the daughter quark. In recent unquenched calculations, the mass of the $\bar{q}q$ pseudoscalar $P_{\bar{q}q}$ lies in the range $0.1m_K^2 \lesssim m_{P_{\bar{q}q}}^2 \lesssim m_K^2$. Second (of special importance in semileptonic decays), the calculations take place in a finite spatial volume, so the 3-momentum takes discrete values. In typical cases the box size $L \approx 2.5$ fm, so the smallest nonzero momentum $\boldsymbol{p}_{(1,0,0)} = 2\pi(1,0,0)/L$ satisfies $|\boldsymbol{p}_{(1,0,0)}| \approx 500$ MeV.

After generating numerical data at several values of $(E, m_{P_{\bar{q}q}}^2)$, the next step for lattice-QCD calculations is to carry out a chiral extrapolation, $m_{P_{\bar{q}q}}^2 \to m_\pi^2$, of the data for $f_\perp$ and $f_\parallel$ [15,16]. The chiral extrapolation must reflect the fact that the form factors are analytic in $E = \sqrt{\boldsymbol{p}^2 + m_P^2}$, not $\boldsymbol{p}$ [17]. Note also that $f_\perp$ and f_+ can be computed only with $\boldsymbol{p} \neq \boldsymbol{0}$, hence $E > m_P$ or, equivalently, $q^2 < q^2_{\rm max}$. The statistical and discretization uncertainties in $f_+(q^2, m_{P_{\bar{q}q}}^2)$ start out smallest at $q^2_{(1,0,0)}$, corresponding to $\boldsymbol{p}_{(1,0,0)}$. A sensible chiral extrapolation will propagate this feature to $f_+(q^2, m_\pi^2)$. Similarly, the statistical and discretization uncertainties in $f_0(q^2, m_\pi^2)$ are smallest near $q^2_{\rm max}$.

When $|\boldsymbol{p}|a$ becomes too large, discretization effects grow out of control. Therefore, the kinematic domain of lattice-QCD calculations is limited to, these days, $|\boldsymbol{p}| \lesssim 1$ GeV, with a corresponding upper limit on E and lower limit on q^2. To extend the form factor over the full physical kinematic domain, a parametrization of the q^2 dependence is needed.

One choice is the Bećirević-Kaidalov (BK) ansatz [18]

$$f_+(q^2) = \frac{F}{(1 - \tilde{q}^2)(1 - \alpha\tilde{q}^2)}, \tag{6}$$

$$f_0(q^2) = \frac{F}{1 - \tilde{q}^2/\beta}, \tag{7}$$

where $\tilde{q}^2 = q^2/m_{H^*}^2$ (H^* is the vector meson of flavor $h\bar{d}$), and F, α, and β are free parameters to be fitted. A key feature of Eq. (6) is the built-in pole at $q^2 = m_{H^*}^2$, or $E = -(m_{H^*}^2 - m_H^2 - m_P^2)/2m_H < 0$, an indisputable feature of the physical f_+. Further singularities at higher negative energy are modeled by the BK parameters α and β. A similar possibility is the Ball-Zwicky (BZ) ansatz [8,19], which has one more parameter for f_+ than BK. A shortcoming of these parametrizations is that comparisons of lattice-QCD and experimental slope parameters can be misleading [20,21], because lattice-QCD slopes are determined near $q^2 = q^2_{\rm max}$, whereas experimental slopes are determined near $q^2 = 0$.

Another approach based on analyticity and unitarity is to write the form factors as

$$f_+(q^2) = \frac{1}{(1 - \tilde{q}^2)\phi_+(q^2)} \sum_{k=0}^{N} a_k z^k, \tag{8}$$

$$f_0(q^2) = \frac{1}{\phi_0(q^2)} \sum_{k=0}^{N} b_k z^k, \tag{9}$$

where $\phi_{+,0}$ are arbitrary, but suitable, functions, and the series coefficients are fit parameters. The variable

$$z = \frac{\sqrt{1 - q^2/t_+} - \sqrt{1 - t_0/t_+}}{\sqrt{1 - q^2/t_+} + \sqrt{1 - t_0/t_+}}, \tag{10}$$

where $t_+ = (m_H + m_P)^2$ and t_0 can be chosen to make $|z|$ small for all kinematically allowed q^2. Like BK and BZ, Eq. (8) builds the H^* pole into f_+, but this approach is model independent because unitarity [17,22,23] and heavy-quark physics [21] impose bounds on $\sum_k |a_k|^2$, $\sum_k |b_k|^2$, and because kinematics set $|z| < 1$. Consequently, the series can be truncated safely, once additional terms are negligible compared to other uncertainties in the analysis.

In all approaches the output of an analysis of lattice-QCD form factors is a fit, usually a two-stage fit of chiral extrapolation followed by q^2 parametrization. Clearly, the final fit describes a curve, and the error matrix of the fit parameters describes an error band. Nevertheless, lattice-QCD results usually have been plotted as a set of points with error bars at fiducial values of q^2 (or E). These points evoke the underlying discrete nature of the 3-momentum $\boldsymbol{p}$ but, in general, the chosen values of q^2 (or E) have nothing to do with the original discrete values of $\boldsymbol{p}$. A plot with a curve plus error band exhibits the same information, while giving a visually superior sense of the correlations between points on the curve.

The experimental measurements of $f_+(q^2)$ come from counting events in bins of q^2 and removing coupling and kinematic factors. The analysis inevitably entails some fitting, to correct for acceptance, etc., but the postfit bins of q^2 faithfully mirror the input to such fits.

If one would like to compare the calculations with the measurements, it is appealing to represent one as a curve with error band, and the other as points with error bars. Bearing the foregoing remarks in mind, it seems natural to draw the curve for lattice-QCD calculations. A few years ago, we prepared illustrative plots for $D \to Kl\nu$ with the Fermilab-MILC [6,7] lattice-QCD calculations and FOCUS [4] and Belle [24] measurements. The intent was pedagogical, and we showed the plots at seminars and conferences [25].

Unfortunately, the error band in that effort was impressionistic, not rigorous. With the prospect of yet-more-precise results based on CLEO-c's full accumulation of 818 pb^{-1} [5], we now present a version that treats the error band as rigorously as possible. We also prepare plots for $D \to \pi l\nu$ and $B \to \pi l\nu$.

As before we shall base the plots for D decays on Ref. [6]. The final result of this analysis consists of the BK parameters (F, α, β) and the 3×3 error matrix. The full statistical error matrix is contained in a detailed, un-

TABLE I. Best-fit values of BK parameters with statistical and systematic errors, successively, in parentheses [6,7,26].

Decay	F	α	β
$D \to Kl\nu$	0.73(3)(7)	0.50(4)(7)	1.31(7)(13)
$D \to \pi l\nu$	0.64(3)(6)	0.44(4)(7)	1.41(6)(7)

TABLE II. Statistical error correlation matrices $\rho_{ij} = \sigma_{ij}^2/(\sigma_{ii}^2\sigma_{jj}^2)^{1/2}$ of the BK parameters [26].

$D \to K$	F	α	β
F	1.000	−0.597	0.530
α	−0.597	1.000	−0.316
β	0.530	−0.316	1.000
$D \to \pi$	F	α	β
F	1.000	−0.583	0.535
α	−0.583	1.000	−0.312
β	0.535	−0.312	1.000

published description of a BK-based analysis of $B \to \pi l\nu$ form factors [26]. The best fit, statistical errors, and systematic errors are tabulated in Table I. The statistical correlation matrices $\rho_{ij} = \sigma_{ij}^2/(\sigma_{ii}^2\sigma_{jj}^2)^{1/2}$ are tabulated in Table II. The correlations among systematic errors are discussed below.

Propagating (correlated) fluctuations in F, α, and β to the form factors, one finds relative squared errors

$$\frac{\sigma_{++}^2}{f_+^2} = \frac{\sigma_{FF}^2}{F^2} + 2\frac{\sigma_{F\alpha}^2}{F}\frac{\tilde{q}^2}{1-\alpha\tilde{q}^2} + \sigma_{\alpha\alpha}^2\left(\frac{\tilde{q}^2}{1-\alpha\tilde{q}^2}\right)^2, \tag{11}$$

$$\frac{\sigma_{00}^2}{f_0^2} = \frac{\sigma_{FF}^2}{F^2} - 2\frac{\sigma_{F\beta}^2}{F\beta}\frac{\tilde{q}^2}{\beta-\tilde{q}^2} + \frac{\sigma_{\beta\beta}^2}{\beta^2}\left(\frac{\tilde{q}^2}{\beta-\tilde{q}^2}\right)^2. \tag{12}$$

These errors are plotted as a function of q^2 in Fig. 1 as solid curves.

The relative statistical errors are smallest for q^2 such that

$$\sigma_{F\alpha}^2 = -F\sigma_{\alpha\alpha}^2\tilde{q}^2/(1-\alpha\tilde{q}^2), \tag{13}$$

$$\sigma_{F\beta}^2 = F\sigma_{\beta\beta}^2\tilde{q}^2/\beta(\beta-\tilde{q}^2). \tag{14}$$

It is illustrative to take $\sigma_{F\alpha}^2$ and $\sigma_{F\beta}^2$ from Tables I and II and solve Eqs. (13) and (14) for $\tilde{q}^2$. We call these values $\tilde{q}_\alpha^2$ and $\tilde{q}_\beta^2$ and tabulate them, as well as $\tilde{q}_{(1,0,0)}^2$ and $\tilde{q}_{\max}^2$, in Table III.

As one can see from Fig. 1 and Table III, the statistical error is smallest between $q_{(1,0,0)}^2$ and $q_{\max}^2$, as expected. One may view this outcome as a check on the fitting procedures.

One can reverse this strategy to determine the correlation between the systematic errors of F and the slope parameters. In the error budget of Ref. [6] the largest

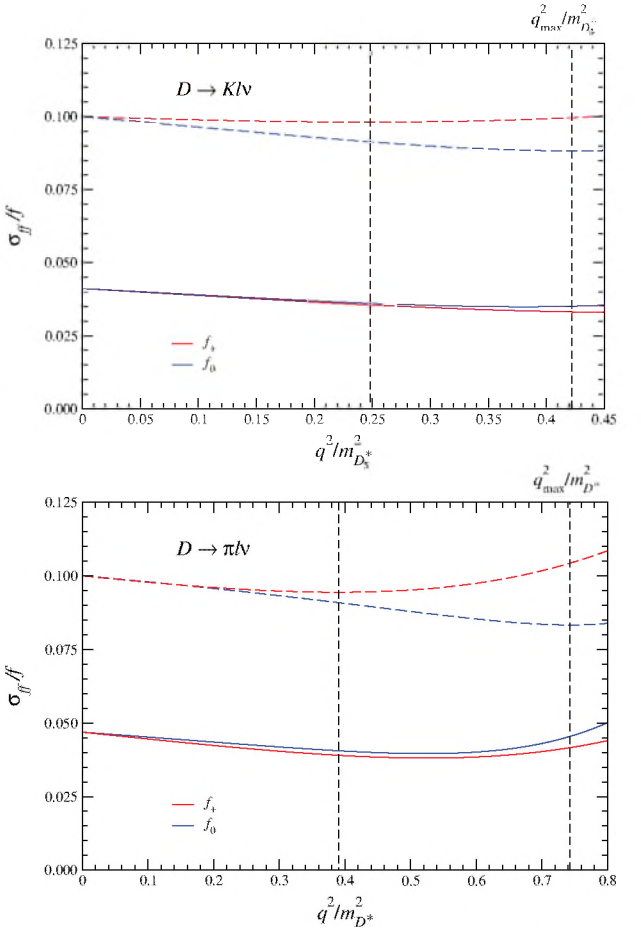

FIG. 1 (color). Relative errors vs q^2. Solid (dashed) curves show the fitted statistical (estimated systematic) error for f_+ (red curves) and f_0 (blue curves). Vertical lines show $q_{(1,0,0)}^2$ and $q_{\max}^2$.

systematic effect comes from discretization errors. These should be smallest around $q_{(1,0,0)}^2$ and $q_{\max}^2$ for f_+ and f_0, respectively, because those correspond to the smallest $|\boldsymbol{p}|$ yielding the respective matrix elements. This yields

$$\rho_{F\alpha}^{\text{syst}} = -0.198(D \to K), \qquad -0.329(D \to \pi), \tag{15}$$

$$\rho_{F\beta}^{\text{syst}} = +0.471(D \to K), \qquad +0.533(D \to \pi), \tag{16}$$

and the dashed curves in Fig. 1.

It is customary to combine statistical and systematic uncertainties by adding the two σ^2 (matrices). Carrying out this procedure leads to the curves and bands in Fig. 2. The error bands seem to contradict the conventional wisdom that the lattice-QCD uncertainties are smallest near $q_{\max}^2$. This is not entirely the case for the *relative* error, as seen in Fig. 1. As q^2 increases, the relative errors decrease until hitting a minimum somewhere between $q_{(1,0,0)}^2$ and $q_{\max}^2$, as is reasonable. The form factors rise faster than the relative errors drop, leading to the increasing absolute error seen in Fig. 2. These features are not an artifact of the BK

TABLE III. Useful quantities for generating and assessing Figs. 1–3.

Decay	H^*	m_{H^*} (MeV)	$E_{(1,0,0)}$ (MeV)	$q^2_{(1,0,0)}$ (GeV^2)	$q^2_{\max}$ (GeV^2)	$\tilde{q}^2_{(1,0,0)}$	$\tilde{q}^2_{\max}$	$\tilde{q}^2_\alpha$	$\tilde{q}^2_\beta$
$D \to Kl\nu$	D_s^*	2112	704	1.10	1.88	0.25	0.42	0.47	0.38
$D \to \pi l\nu$	D^*	2008	518	1.57	3.00	0.39	0.74	0.53	0.52
$B \to \pi l\nu$	B^*	5325	518	22.4	26.4	0.79	0.93	...	...

parametrization, as we shall see below with the $B \to \pi l\nu$ form factor f_+.

Figure 2 is the first main result of this article. It shows the form factors f_+ and f_0 for $D \to Kl\nu$ and $D \to \pi l\nu$. The lattice-QCD results are shown as curves (red for f_+, blue for f_0) with two errors bands, one statistical (orange for f_+, gray for f_0), the other systematic and statistical combined (yellow for f_+, light blue for f_0). Experimental measurements for f_+ [24,27–29] are overlaid as points with error bars. It may require careful scrutiny to see which experiment is which, but a glance reveals how well the points and curves agree. The agreement is good for $D \to \pi l\nu$ and very good for $D \to Kl\nu$.

For the z expansion the propagation of errors is even simpler. Focusing on f_+, one has from Eq. (8)

$$\frac{\sigma^2_{++}}{f_+^2} = \frac{\sum_{k,l=0}^{N} \sigma^2_{kl} z^{k+l}}{[\sum_{k=0}^{N} a_k z^k]^2}, \tag{17}$$

where the indices on σ^2 correspond to those on the series coefficients. The coefficients and error matrix for the $N = 3$ fit ($t_0 = 0.65 q^2_{\max}$) are tabulated in Table IV.

The z-series fit was carried out after assigning q^2-dependent systematic uncertainties, so Table IV refers

TABLE IV. Best-fit values a_k and correlation matrix ρ_{kl} of the 3-term z expansion of f_+ for $B \to \pi l\nu$, with statistical and systematic errors combined [9].

Fit:	0.0216(27)	−0.0378(191)	−0.113(27)
ρ	a_0	a_1	a_2
a_0	1.000	0.640	0.475
a_1	0.640	1.000	0.964
a_2	0.474	0.964	1.000

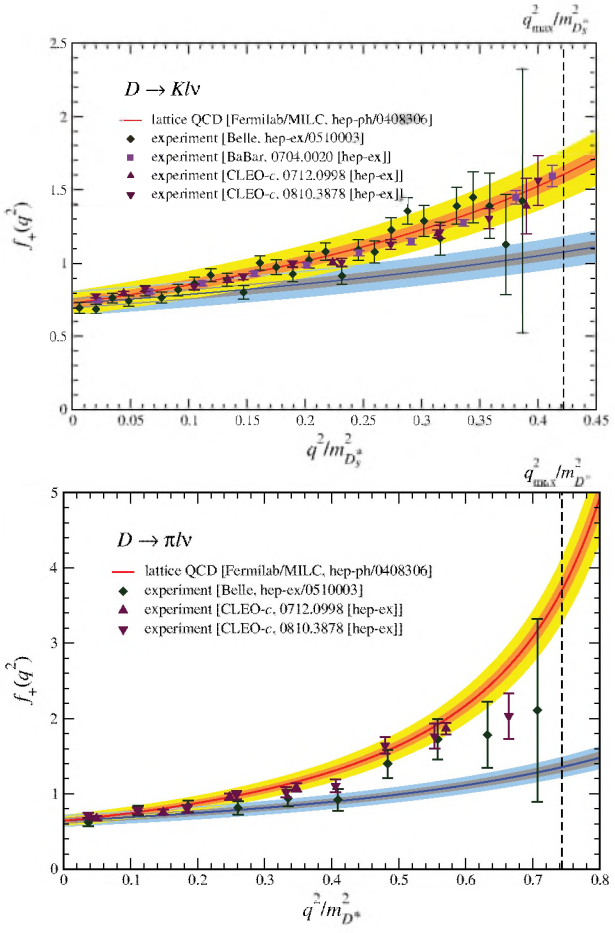

FIG. 2 (color). Form factors f_+ (and f_0) for semileptonic D decays, from lattice QCD [6,26], expressed as a red (blue) curve with an orange (gray) statistical error band and a yellow (light blue) combined error band. Error bands take correlations into account. Measurements of f_+ are from Belle (green diamonds) [24], *BABAR* (magenta squares) [27], and CLEO-c (maroon triangles) [28,29]. The vertical line shows $q^2_{\max}$.

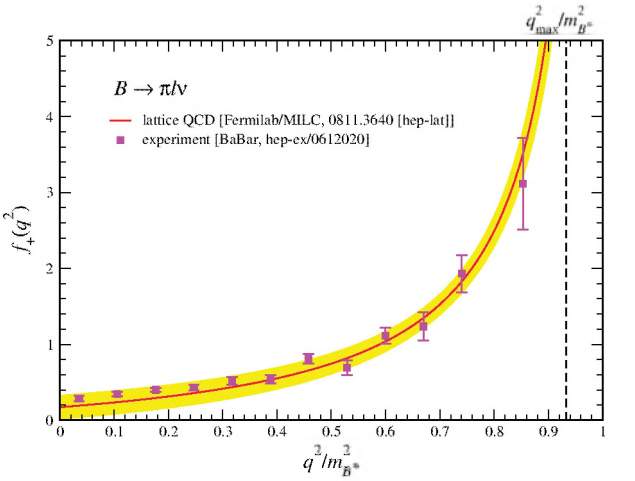

FIG. 3 (color). Form factor f_+ for $B \to \pi l\nu$ expressed as a curve (red) from the best fit with a total error band (yellow) from taking correlations in the fit parameters into account [9], overlaid with measurements of $|V_{ub}|f_+/(3.38 \times 10^{-3})$ from *BABAR* (magenta squares) [30]. The vertical line shows $q^2_{\max}$.

to the combined statistical and systematic errors of this analysis.

This information, combined with the outer function ϕ_+ [9], is used to produce Fig. 3, the second main result of this paper. Now the curve and error band conform with preconceptions, for several reasons. First, $q^2_{(1,0,0)}$ is close to $q^2_{\rm max}$, rather than in the middle of the kinematic range. Second, the chiral extrapolation in Ref. [9] is less aggressive than that in Ref. [6], leading to a larger but more realistic error at $q^2 = 0$. The most striking aspect is that even though the absolute error in f_+ is increasing for $\vec{q}^2 \geq 0.8$, the band remains narrow. The band simply conveys the point-to-point correlations better.

This paper shows in detail how to compare semileptonic form factors from lattice QCD and from experiments. For illustration we use the BK parametrization for $D \to Kl\nu$ and $D \to \pi l\nu$, and the z expansion for $B \to \pi l\nu$. Clearly, the idea is more general. For example, an interesting prospect relevant to semileptonic form factors is to inject 3-momenta smaller that $\boldsymbol{p}_{(1,0,0)}$ using "twisted" boundary conditions [31–33]. That strategy should improve the accuracy of parameters in the chiral extrapolation and, hence, the BK, BZ, or z fits. The output of any fit could still be exhibited as outlined here, although one should bear in mind that superior visualization of a fitting procedure does not repair any shortcomings of the fit itself.

We would like to thank Ian Shipsey for encouraging us to think carefully about the correlations in the systematic errors. We would like to thank Laurenz Widhalm for providing the Belle data in numerical form [24], and Shipsey for the *BABAR* and CLEO D-decay data [27–29]. Computations for this work were carried out in part on facilities of the USQCD Collaboration, which are funded by the Office of Science of the United States Department of Energy. This work was supported in part by the U.S. Department of Energy under Grants No. DE-FC02-06ER41446 (C. D., L. L., M. B. O.), No. DE-FG02-91ER40661 (S. G.), No. DE-FG02-91ER40677 (A. X. E-K., R. T. E., E. G.), No. DE-FG02-91ER40628 (C. B., J. L.), and No. DE-FG02-04ER41298 (D. T.); by the National Science Foundation under Grants No. PHY-0555243, No. PHY-0757333, No. PHY-0703296 (C. D., L. L., M. B. O.), No. PHY-0555235 (J. L.), and No. PHY-0757035 (R. S.); and by Universities Research Associates (R. T. E., E. G.). This manuscript has been coauthored by an employee of Brookhaven Science Associates, LLC, under Contract No. DE-AC02-98CH10886 with the U.S. Department of Energy. Fermilab is operated by Fermi Research Alliance, LLC, under Contract No. DE-AC02-07CH11359 with the U.S. Department of Energy.

[1] M. Ablikim *et al.* (BES Collaboration), Phys. Lett. B **597**, 39 (2004).
[2] G. S. Huang *et al.* (CLEO Collaboration), Phys. Rev. Lett. **94**, 011802 (2005).
[3] J. M. Link *et al.* (FOCUS Collaboration), Phys. Lett. B **607**, 51 (2005).
[4] J. M. Link *et al.* (FOCUS Collaboration), Phys. Lett. B **607**, 233 (2005).
[5] D. Besson *et al.* (CLEO Collaboration), Phys. Rev. D **80**, 032005 (2009).
[6] C. Aubin *et al.* (Fermilab Lattice, MILC, and HPQCD Collaborations), Phys. Rev. Lett. **94**, 011601 (2005).
[7] M. Okamoto *et al.* (Fermilab Lattice, MILC, and HPQCD Collaborations), Nucl. Phys. B, Proc. Suppl. **140**, 461 (2005).
[8] E. Dalgic neé Gulez *et al.* (HPQCD Collaboration), Phys. Rev. D **73**, 074502 (2006); **75**, 119906(E) (2007).
[9] J. A. Bailey *et al.*, Phys. Rev. D **79**, 054507 (2009).
[10] K. C. Bowler *et al.* (UKQCD Collaboration), Phys. Lett. B **486**, 111 (2000).
[11] A. Abada *et al.*, Nucl. Phys. **B619**, 565 (2001).
[12] A. X. El-Khadra *et al.*, Phys. Rev. D **64**, 014502 (2001).
[13] S. Aoki *et al.* (JLQCD Collaboration), Phys. Rev. D **64**, 114505 (2001).
[14] J. Shigemitsu *et al.*, Phys. Rev. D **66**, 074506 (2002).
[15] D. Bećirević, S. Prelovšek, and J. Zupan, Phys. Rev. D **67**, 054010 (2003).
[16] C. Aubin and C. Bernard, Phys. Rev. D **76**, 014002 (2007).
[17] L. Lellouch, Nucl. Phys. **B479**, 353 (1996).
[18] D. Bećirević and A. B. Kaidalov, Phys. Lett. B **478**, 417 (2000).
[19] P. Ball and R. Zwicky, Phys. Rev. D **71**, 014015 (2005).
[20] R. J. Hill, Phys. Rev. D **73**, 014012 (2006).
[21] T. Becher and R. J. Hill, Phys. Lett. B **633**, 61 (2006).
[22] C. Bourrely, B. Machet, and E. de Rafael, Nucl. Phys. **B189**, 157 (1981).
[23] C. G. Boyd, B. Grinstein, and R. F. Lebed, Phys. Rev. Lett. **74**, 4603 (1995); C. G. Boyd and M. J. Savage, Phys. Rev. D **56**, 303 (1997).
[24] L. Widhalm *et al.* (Belle Collaboration), Phys. Rev. Lett. **97**, 061804 (2006); K. Abe *et al.* (Belle Collaboration), arXiv:hep-ex/0510003.
[25] A. S. Kronfeld *et al.* (Fermilab Lattice, MILC, and HPQCD Collaborations), Proc. Sci., LAT2005 (2006) 206; Int. J. Mod. Phys. A **21**, 713 (2006); A. S. Kronfeld (Fermilab Lattice, MILC, and HPQCD Collaborations), J. Phys. Conf. Ser. **46**, 147 (2006).
[26] M. Okamoto (Fermilab Lattice and MILC Collaborations) (unpublished). A public report of this work is contained in Ref. [7]. This line of analysis was superseded by Ref. [9].

[27] B. Aubert *et al.* (*BABAR* Collaboration), Phys. Rev. D **76**, 052005 (2007).
[28] D. Cronin-Hennessy *et al.* (CLEO Collaboration), Phys. Rev. Lett. **100**, 251802 (2008); S. Dobbs *et al.* (CLEO Collaboration), Phys. Rev. D **77**, 112005 (2008).
[29] J. Y. Ge *et al.* (CLEO Collaboration), Phys. Rev. D **79**, 052010 (2009).
[30] B. Aubert *et al.* (*BABAR* Collaboration), Phys. Rev. Lett. **98**, 091801 (2007).
[31] P. F. Bedaque, Phys. Lett. B **593**, 82 (2004).
[32] C. T. Sachrajda and G. Villadoro, Phys. Lett. B **609**, 73 (2005).
[33] J. M. Flynn, A. Jüttner, and C. T. Sachrajda (UKQCD Collaboration), Phys. Lett. B **632**, 313 (2006).